Chun-yu Wang, Yu-huan Bu*, Hua-jie Liu and Sheng-lai Guo

Preparation and characterization of core-shell oil absorption materials stabilized by modified fumed silica

DOI 10.1515/polyeng-2016-0075
Received February 23, 2016; accepted July 3, 2016; previously published online August 17, 2016

Abstract: The core-shell oil absorption material (OAM) with fumed silica shell was achieved from Pickering polymerization. The modified fumed silica wall could well stabilize both Pickering emulsion and Pickering polymerization. The particle size of encapsulated OAMs decreased with the increasing concentration of fumed silica and remained unchanged when the concentration was more than 1 wt.%. This fumed silica shell had little effect on the oil absorption rate of OAM. The importance was that the shell reversed the surface property and improved the alkali resistance of OAM. We believe that our core-shell OAMs could reach the self-healing ability of the oil well cement.

Keywords: alkali resistance; fumed silica; oil absorption materials; Pickering polymerization.

1 Introduction

Oil absorption materials (OAMs), which can absorb oil from water, store a large volume of oil, and swell after absorbing oil, have attracted considerable attention in recent years. OAMs (e.g. polyacrylate [1–3], polyolefin stretched tape [4], and rubber [5–7]) have been widely used in environmental protection [1, 5, 7, 8], controlled release base materials [9, 10], filter additives [11], sealant materials [12], and so on. Among these familiar OAMs, the most important group is polyacrylate, which is easily available and inexpensive and has clear oil/water selectivity, fast absorption rate, and high oil retention. Having these outstanding characteristics, polyacrylate and its ramification is widely used in more fields.

***Corresponding author: Yu-huan Bu,** College of Petroleum Engineering, China University of Petroleum, Qingdao 266580, China, e-mail: buyuhuan@163.com
Chun-yu Wang, Hua-jie Liu and Sheng-lai Guo: College of Petroleum Engineering, China University of Petroleum, Qingdao 266580, China

One promising use of polyacrylate OAMs is their application in oil well cement to realize the self-healing property when microcracks are formed in cement paste. It is known as self-healing cement (SHC) [13–17]. Because oil well cement slurry is hydrophilic and alkaline [18] and polyacrylate OAMs are hydrophobic and easy alkaline hydrolyzing [19], polyacrylate OAMs are hard to be employed directly in oil well cement. On the one hand, the oil absorption rate of OAMs would lessen if polyacrylate OAMs were alkaline hydrolysis; on the other hand, the cement paste would not self-heal microcracks if polyacrylate OAMs had bad dispersion in cement.

To improve the applicability of polyacrylate OAMs in cement, the surface property should be reversed and alkali resistance should be improved. Microsphere-shaped OAMs are easy to adjust. There are several methods that can prepare microspheres. Microemulsion polymerization has a stable reaction process [3]; however, particles are too small to be used in cement. A larger particle size can be realized from suspension polymerization [1]. However, the reaction process is not stable while using hydroxylethyl cellulose, gelatin, or sodium dodecyl benzene sulfonate as dispersing agents at high temperature [20]. A new polymerization method called Pickering polymerization [21] has attracted more and more attention in recent years. The method is stabilized by solid particles instead of molecular surfactants and is a template to prepare core-shell microspheres. It may be effective to solve the stability problem in preparing microsphere-shaped OAMs and its applicability in cement.

In the past, some inorganic particles have already been used as a stabilizer of Pickering polymerization [22–29]. To apply core-shell OAM microspheres to cement, fumed silica is employed as a stabilizer to produce microspheres. This is because fumed silica is amorphous [30] and cement slurry is alkaline, so fumed silica can react with cement slurry [31] and strengthen the combination between organic polyacrylates and inorganic cement. Most studies used nanometer silica to stabilize Pickering emulsion and droplets were in the micron level [25–28]. This paper introduced microsilica to obtain larger oil droplets and larger OAM microspheres eventually. Pure

fumed silica is completely hydrophilic, and it cannot self-absorb on the oil/water interface [32–34]. However, fumed silica modified by a silane coupling agent is partly hydrophobic and can stabilize oil-in-water Pickering emulsion [35].

In this study, we prepared core-shell OAM microspheres with quite a stable process and a fumed silica shell from Pickering emulsion template, which could improve both the alkali resistance of OAMs and dispersability in cement slurries. Modified fumed silica could stabilize Pickering polymerization, and we analyzed the "protective effect" of modified fumed silica in this process. There was a shell on the surface of OAM microspheres, and we studied how it affected the oil absorption rate of OAMs. Because fumed silica could react with alkali liquor, we analyzed the effect of fumed silica shell on the improvement of alkali resistance of core-shell OAM microspheres. At last, we compared the contact angle of polyacrylates and core-shell polyacrylate microspheres to explain the good dispersion of microspheres in cement slurry.

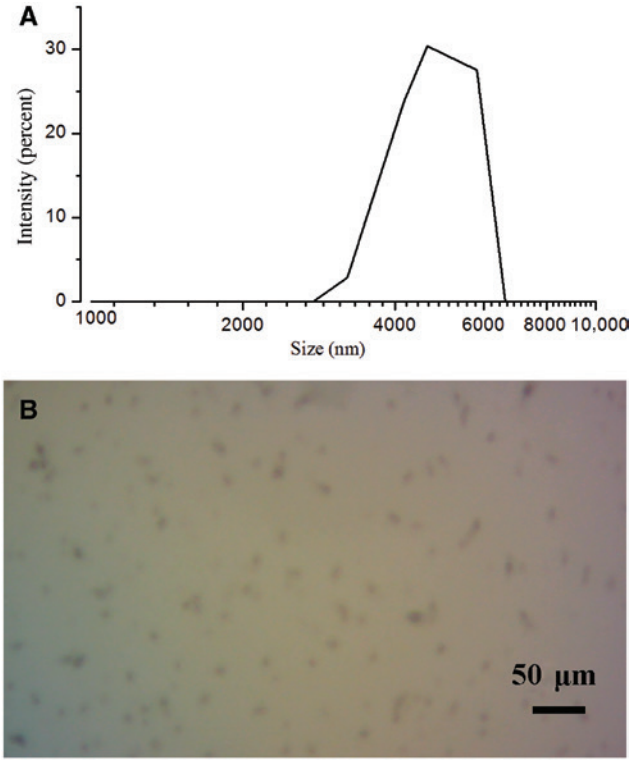

Figure 1: Characteristics of modified fumed silica: laser diffraction particle size distribution curves (A) and optical micrograph (B).

2 Materials and methods

2.1 Materials

Methyl methacrylate (MMA; 98%; purchased from Sinopharm Chemical Reagent Co., Ltd., Shanghai, China) and lauryl methacrylate (LMA; 95%; purchased from Aladdin Industrial Corp., Shanghai, China) were used as monomers. Divinylbenzene (DVB; 55%; obtained from Aladdin Industrial) was used as a cross-linking agent. Benzoyl peroxide (BPO; 98%; J&K Scientific Ltd., Beijing, China) was used as initiator. Ethyl acetate (EA; 99.5%; purchased from Sinopharm Chemical Reagent) was used to make pores. Toluene (99%; purchased from Sinopharm Chemical Reagent) was used to test the oil absorption rate of OAMs. Gelatin (chemical pure) was purchased from Aladdin Industrial. Deionized water was used throughout the experiments.

Modified fumed silica particles were provided by Suzhou Huize Fine Chemical Co., Ltd. (Suzhou, China). The wettability of fumed silica particles was neutral and the median diameter was 4.63 μm (Figure 1A) as measured by Malvern Zetasizer NanoZS (Malvern, UK). The morphology of the modified fumed silica was investigated by an optical microscope (Figure 1B).

2.2 Synthesis of core-shell OAM microspheres

Core-shell OAM microspheres were prepared by Pickering polymerization, and the synthesis process was as follows: 200 g deionized water was put into a 500 ml three-mouth flask, and a certain quality of modified fumed silica (2 g) was added in the flask and the mixture was stirred well. Then, a suitable amount of component (5.5 g MMA and 7 g LMA) was put into a beaker, wherein a cross-linking agent (0.06 g DVB), an initiator (0.2 g BPO), and a pore-forming agent (12.5 g EA) were added in sequence, and all of the compositions were stirred until the initiator (BPO) was completely dissolved. Then, the evenly stirred oil phase was dropped into the water phase at a stirring rate of 1000 rpm, and the stirring rate was slowed down to 300 rpm 10 min later after the oil phase was totally dropped into the water phase. The water bath temperature was set to 85°C and the reaction time was set to 150 min. Core-shell OAM microspheres were filtered after the reaction and washed three times with deionized water at 80°C. Finally, the microspheres were dried at 80°C for 24 h to vaporize water and EA.

2.3 Scanning electron microscope (SEM)

The morphology of core-shell OAM microspheres was observed under an S-4800 cold field emission scanning electron microscope (SEM). The microspheres were sprayed with gold before the test. SEM analyses were conducted at the State Key Laboratory of Heavy Oil Research at the China University of Petroleum (East China).

2.4 Fourier transform infrared (FTIR) spectrometry

FTIR spectra of core-shell OAM microspheres were recorded on a Bio-Rad FTS135 FTIR spectroscope at the State Key Laboratory of Heavy Oil Research at the China University of Petroleum. The test conditions were potassium bromide pellets and wavelength range of 4000 to 400 cm^{-1}.

2.5 Particle size distribution test

The particle size distribution of core-shell OAM microspheres was tested using Bettersize 2000 laser particle distribution instrument. Particles were dispersed in deionized water before the test and the concentration was 1 wt.%.

2.6 Oil absorption test

Because the cement slurry is alkaline and the pH value is approximately 13, core-shell OAM microspheres were alkali treated at 75°C and pH 13 for 300 min. Then, the oil absorption rates of the microspheres before and after alkali treatment were tested in toluene at 75°C. The measurement procedure was as follows: microspheres with a quantity of W_1 were placed into a nylon bag. The quantity of microspheres and nylon bag was weighed and the value was denoted as W_2. The nylon bag was put into toluene at 75°C. After 24 h, the nylon bag was taken out and suspended until no droplet is dripping. Then, the nylon bag was weighed again and the value was denoted as W_3. The oil absorption rate of microspheres is given by

$$G=(W_3-W_2)/W_1 \quad (1)$$

where G is the oil absorption rate of OAMs (g/g).

2.7 Contact angle test

The contact angle can directly reflect the hydrophilicity or lipophilicity of core-shell OAM microspheres and indirectly explain their dispersion in cement slurry. The contact angles of microspheres synthesized using gelatin or fumed silica particles as dispersant were tested. Kostakis et al. [36] and Yang et al. [37] provided methods for testing the contact angle of powder. The method used in this paper was as follows: OAMs (0.5 g) were put into a compression molding device and compressed under a pressure of 5 MPa for 1 min into a test piece with a diameter of 15 mm and a thickness of 2 mm. The contact angle of the test piece was tested using PDE-1700 contact angle meter (KRÜSS Co., Ltd., Hamburg, Germany).

3 Results and discussion

3.1 Pickering polymerization stabilized by modified fumed silica

The Pickering polymerization of core-shell OAM microspheres had two stages: dispersion stage and encapsulation stage. The dispersion stage corresponded to the high-speed stirring stage and lasted 10 min, whereas the encapsulation stage, which is also known as the polymerization stage, corresponded to the low-speed stirring stage and lasted 150 min.

The oil phase contained a monomer (MMA and LMA), a pore-forming agent (EA), a cross-linking agent (DVB), and an initiator (BPO). In the dispersion stage, the oil phase was cut into oil droplets under the given stirring rate. Fumed silica particles were absorbed on the oil/water interface and prevented the droplets from coalescence. This stage is the formation of Pickering emulsion. Interface adsorption energy is a quantity that reflects the reduction of interface energy when inorganic particles are adsorbed on the oil/water interface. For a spherical particle with radius R, its interface adsorption energy formula is [38, 39]

$$E=\pi R^2\gamma_{OW}(1\pm\cos\theta)^2 \quad (2)$$

where E is the interface adsorption energy ($\times10^{-8}$ J), R is the radius of a spherical particle (nm), γ_{OW} is the interfacial tension between oil and water (N/m), and θ is the contact angle of the particle. When the particle diffuses into the water, the sign in parentheses is negative; on the contrary, the sign is positive.

Binks and Lumsdon [40] studied the interface adsorption energy of a spherical particle (R=1×10^{-8} nm) at a planar oil/water interface changed with the contact angle θ. The results showed that the interface adsorption energy

E was much higher than the energy of thermal motion k_BT (where k_B is the Boltzmann constant and T is the thermodynamic temperature) when the contact angle θ was 90°. In this paper, fumed silica was modified by a silane coupling agent and the contact angle was a little <90°. Therefore, the adsorption of modified fumed silica was irreversible, and Pickering emulsion was prepared.

Figure 2A shows the Pickering emulsion under static condition after 10 min of high-speed stirring. Two layers were formed: the upper layer was the layer of oil droplets suspended in water and the lower layer was the layer of water phase containing fumed silica particles. Therefore, fumed silica particles were not totally adsorbed on the oil/water interface, and there were quite a lot of particles suspended in the aqueous phase. Frelichowska et al. [41] used to analyze the presence of excess silica coexisting with oil droplets in the emulsion by ultracentrifugation and infrared absorption spectroscopy. The excess fumed silica in the bulk phase could form a three-dimensional network surrounding the droplets [42–44], which prevented droplets from coalescence. The larger interface adsorption energy and the three-dimensional network of fumed silica were the two main factors that stabilized Pickering emulsion.

During polymerization, the monomer (MMA and LMA) was polymerized in the presence of BPO and then formed short-chain molecules. As time went by, short-chain molecules formed long-chain molecules and cross-linked by DVB and then formed a space network structure. Cheng et al. [45] found that nanocomposites could combine with the polymer because of attractive interactions, and the static thickness of the interfacial layer was found to increase with the molecular weight. Therefore, fumed silica particles would form a shell layer around the polymer. On the contrary, the viscosity of the oil phase was increasing during the stage, and solid microspheres were created at last.

As shown in Figure 2, it is clear that extra fumed silica particles suspended in the aqueous phase were reduced from the start to 25 min, and the aqueous phase became clear at 25 min. This means that fumed silica particles were constantly absorbed on the oil/water interface. This phenomenon was analyzed by the deformation of droplets and the viscosity of the oil phase.

Experiments [41] have shown that, under the same mechanical strength, the interfacial area per unit mass of silica was larger when the oil phase had a low viscosity than when the oil phase had a high viscosity. For the polymerization stage, the viscosity of the oil phase increased with time. At the beginning, Pickering emulsion had a large interfacial area per unit mass of silica, and then interfacial area should decrease with increasing viscosity of the oil phase. That is to say, fumed silica particles would desorb from the oil/water interface. However, the desorption described by Eq. (2) is not possible.

The oil droplets suspended in the aqueous phase are not always spherical. They are easy to deform in stirring. It is well known that a spherical oil droplet has the minimum oil/water interface compared to any other shape at the same volume. Therefore, the oil/water interface would increase after the deformation of droplets (Figure 3C and F). Binks and Whitby [46] found that the droplets of viscous silicone oil did not find it easy to go back to a spherical shape after their deformation in strong shearing. Therefore, the new oil/water interface was formed constantly during the polymerization stage, and it led extra fumed silica particles in aqueous phase adsorb on the interface to reduce the interfacial tension (Figure 3D and G). When the droplets relaxed

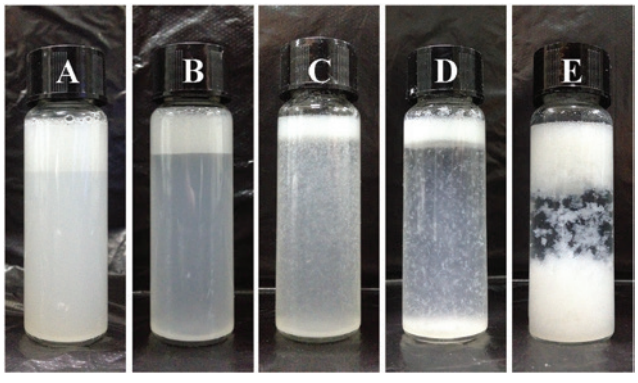

Figure 2: Photographs of Pickering emulsion samples at different times: (A) 0 min, (B) 7 min, (C) 15 min, (D) 20 min, and (E) 25 min of the polymerization stage.
The samples were allowed to stand for 2 min at room temperature.

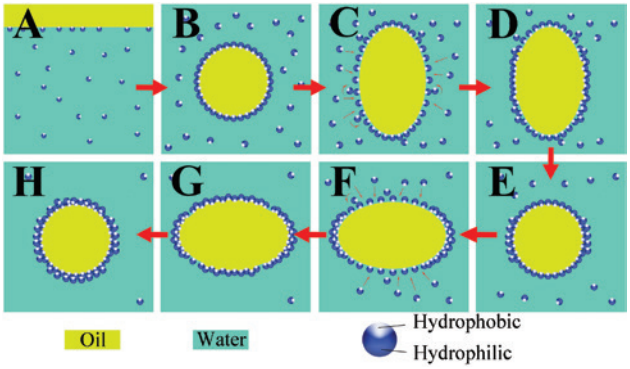

Figure 3: Schematic illustration of the preparation of core-shell OAM microspheres with fumed silica shell based on Pickering polymerization.

back to spherical phase, their surfaces would reduce and fumed silica particles stacked together to form multilayers (Figure 3E and H). Unlike Pickering emulsion, extra fumed silica particles decreased or even dispersed in Pickering polymerization as time went by. This phenomenon could prevent viscous droplets from adhesion and coalescence, and it could stabilize the polymerization stage from the beginning to the end.

During the encapsulation stage, fumed silica particles were constantly absorbed on the oil/water interface and combined with the inner polymer to form the shell layer. Because cement is an inorganic material, this layer would well improve the applicability of OAM in cement and increase the combination capacity between organic OAM and inorganic cement.

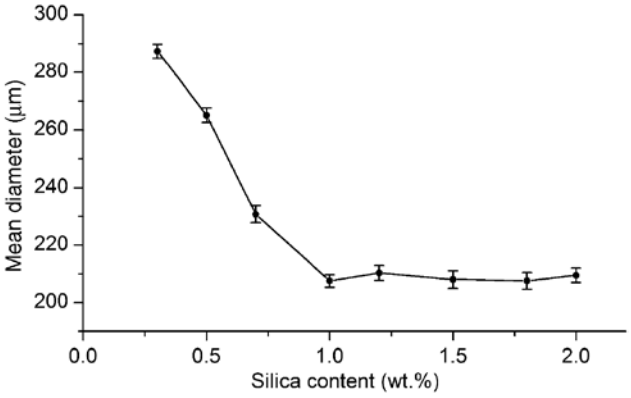

Figure 5: Relationship between silica content and mean diameter of core-shell OAM microspheres.

3.2 Particle size of core-shell OAMs

The concentration of silica particles in the bulk phase and the amount of oil phase are the two factors that influenced the droplet size [46, 47] and determined the size of core-shell OAM microspheres. The concentrations of fumed silica in the aqueous phase varied from 0.3 to 2 wt.%, and the ratio of oil to water was 12.5 wt.%. When the amount of silica was lower than 0.3 wt.%, Pickering emulsion was not stable and droplets were easy to adhere during polymerization.

Having more stable polymerization process, core-shell OAM microspheres had a narrow particle size distribution (Figure 4). As shown in Figure 5, the particle size of microspheres is reduced when the amount of fumed silica is 0.3 to 1 wt.%. It stops reducing when the amount is larger than 1 wt.% and reaches a plateau. For Pickering emulsion, Wiley [48] and Arditty et al. [49–51] have studied that the droplet size is reduced as the amount of particles increases. However, this trend would not last. Midmore [52] and Abend et al. [42] also observed a "plateau" in the silica concentration range. This is because the emulsification process needs energy to shear the oil droplets to smaller size, but ultrasonic dispersion could not provide enough energy. For Pickering polymerization, it is the same. With a large amount of fumed silica, there is a limit particle size for core-shell OAM microspheres under stirring condition.

3.3 FTIR test

FTIR spectra were used to verify whether core-shell OAM microspheres contained silica. We prepared two kinds of OAMs: one used fumed silica as dispersant and the concentration was 2 wt.% (Figure 6B) and the other used gelatin as dispersant and the concentration was 1 wt.% (Figure 6A).

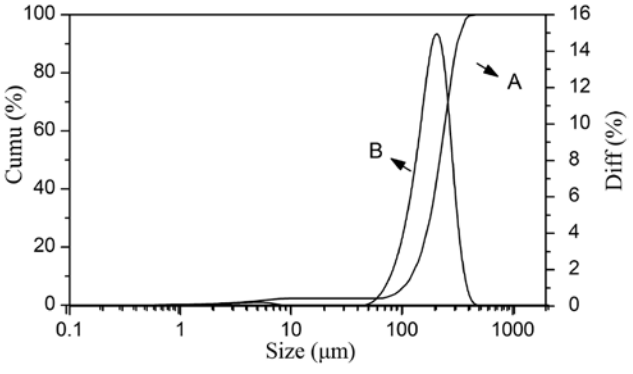

Figure 4: Particle size distribution curves: (A) cumulative distribution and (B) difference distribution.
The concentration of fumed silica used for preparing core-shell OAM microspheres was 1%.

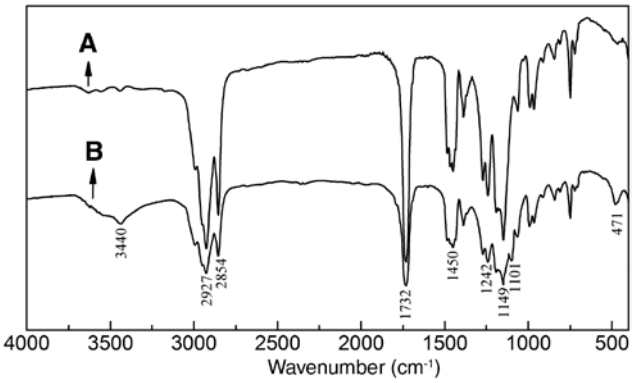

Figure 6: FTIR spectra of polyacrylate (A) and core-shell OAM microspheres (B).

Analyzing the peaks of the two curves (Figure 6A and B), the characteristic absorption band at 2927 cm^{-1} corresponds to the aliphatic C-H bond and unsymmetrical stretching vibrations of $-CH_3$ groups, and the characteristic absorption band at 2854 cm^{-1} is due to the aliphatic C-H symmetrical stretching vibrations of $-CH_2$ groups of the 11 $-CH_2$ of LMA. It is clear that there is a characteristic absorption peak of the asymmetric bending vibrations of C-H at 1450 cm^{-1}, the characteristic absorption band of C=O appears at 1732 cm^{-1}, and that of C-O-C appears at 1149 and 1242 cm^{-1}. These characteristic absorption peaks confirmed that MMA and LMA are in a copolymerization reaction with OAMs. However, from the FTIR spectra of core-shell OAM microspheres, the characteristic absorption bands at 1101 and 471 cm^{-1} are the characteristic absorption bands of SiO_2. It confirms that core-shell OAM microspheres are a composite polymer of SiO_2, MMA, and LMA.

3.4 Micromorphology

To explain the role played by fumed silica particles in the preparation process, two kinds of OAMs using fumed silica particles and gelatin as dispersant, respectively, were analyzed by SEM. Microspheres using fumed silica particles as dispersant do not adhere together and have high sphericity (Figure 7C). However, microspheres using gelatin as dispersant do not have the same properties, and the microspheres in different sizes cohere together (Figure 7A). Thus, it is clear that fumed silica particles play a more effective role than gelatin in polymerization. On the one hand, fumed silica particles can stabilize the polymerization process; on the other hand, they can make the particle size of microspheres uniform. As shown in Figure 7D, there is a fumed silica shell on the surface of microspheres using fumed silica particles as dispersant, whereas there is no shell on the surface of microspheres using gelatin

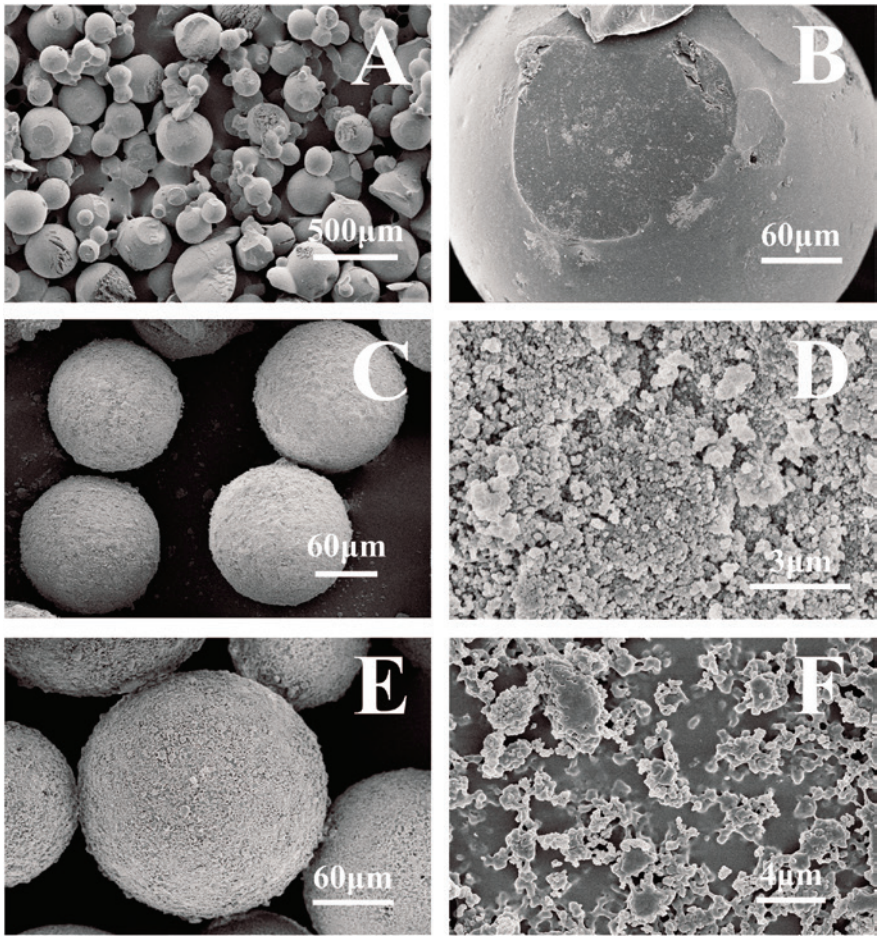

Figure 7: SEM images of polyacrylate microspheres (A and B) and core-shell OAM microspheres before alkali treatment (C and D) and after alkali treatment (E and F).
Core-shell OAM microspheres were alkali treated under 75°C.

as dispersant as shown in Figure 7B. This illustrates the combination of fumed silica shell and the inner core and the preparation of core-shell OAM microspheres.

3.5 Oil absorption rate

The oil absorption test was used to evaluate whether fumed silica shell affects the oil absorption performance of core-shell OAM microspheres. In this experiment, 1 wt.% concentration of fumed silica was used for core-shell OAMs microspheres, whereas 1 wt.% concentration of gelatin was used for the other kind of OAMs. The concentration of the pore-forming agent (EA) varied from 0 to 150 wt% relating to the total mass of monomer (MMA and LMA). Because polyacrylate microspheres using gelatin as dispersant coalesced together and the particle size was uneven, the lumps were dried and smashed, and the oil absorption rate was measured using particles of 150–250 μm.

As shown in Figure 8, the oil absorption rate of the two kinds of OAMs is close, and this explains that the kind of dispersing agent has little effect on the oil absorption rate. However, the oil absorption rate of core-shell OAM microspheres is smaller than polyacrylate microspheres overall. This is because fumed silica multilayer shells combined with the inner core and limited the swelling of polyacrylate while absorbing oil.

3.6 Alkali resistance

To measure the alkali resistance of OAMs, the oil absorption rates of OAMs using gelatin and fumed silica as dispersing agent were tested after alkali (pH 13) treatment at 75°C for 300 min and compared to that before alkali treatment (Figures 9 and 10). The oil absorption rate of core-shell OAM microspheres after alkali treatment is higher than before treatment (Figure 9). This is because fumed silica shell on the surface of microspheres can react with alkali liquor and dissolve. Therefore, the limitation of fumed silica shell on the expansion of core-shell OAM microspheres was relieved partly while absorbing oil. The oil absorption rate of polyacrylate microspheres after alkali treatment is lower than before treatment (Figure 10). This illustrates the hydrolysis reaction of polyacrylate in an environment and that the structure of the polyacrylate was destroyed. Due to the existence of fumed silica shell, which prevented the inner polyacrylate core from contacting alkali liquor, the alkali resistance of core-shell OAM microspheres using fumed silica particles as dispersant was stronger than polyacrylate using gelatin as dispersant. This explained that core-shell OAM microspheres can be used directly in cement slurry downhole.

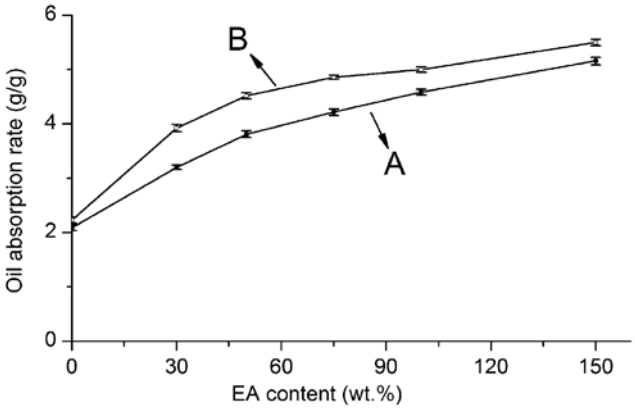

Figure 9: Change of oil absorption rate of core-shell OAM microspheres before alkali treatment (A) and after alkali treatment (B).

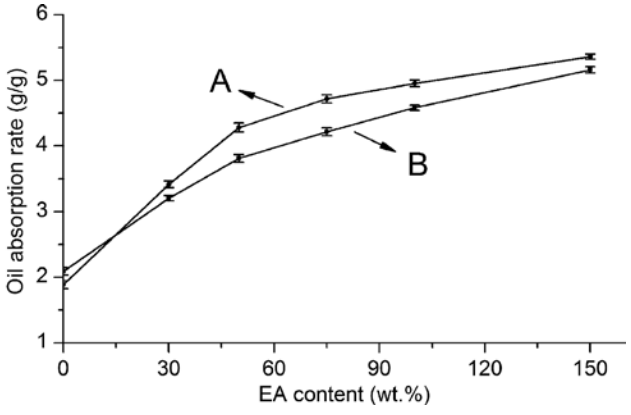

Figure 8: Relationship between EA content and oil absorption rate of polyacrylate microspheres (A) and core-shell OAM microspheres (B).

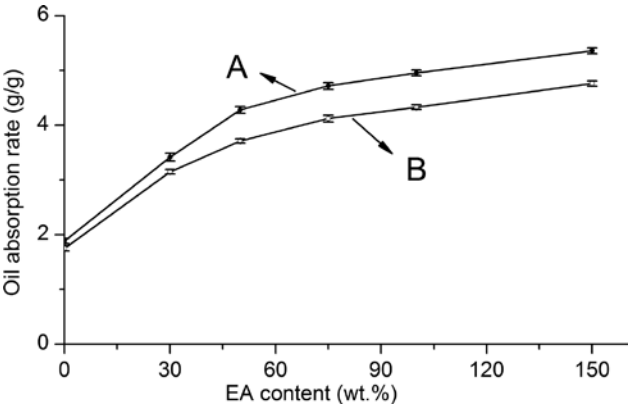

Figure 10: Change of oil absorption rate of polyacrylate microspheres before alkali treatment (A) and after alkali treatment (B).

Besides, the oil absorption rate of OAMs is mainly controlled by the amount of EA and is increased with the increasing amount of EA (Figures 8–10). It is because the space grid structure of polyacrylate is controlled by the amount of the pore-forming agent and is an important factor that affects the oil absorption rate of OAMs [53].

SEM was used to analyze the variation of the surface morphology of core-shell OAM microspheres before and after alkali treatment. The fumed silica shell was partly dissolved after alkali treatment (compare Figure 7D to F). This is because fumed silica was amorphous and could react with alkali liquor at high temperature [30]. However, fumed silica formed multilayer shells on the surface of polyacrylate microspheres, and the shells were too strong to be totally dissolved in alkali liquor. The multilayer shells provided a barrier between the inner polyacrylate core and the alkali liquor and prevented polyacrylate from hydrolyzing.

3.7 Contact angle

The cement slurry is hydrophilic, but the polyacrylate microspheres synthesized using conventional methods are lipophilic. Therefore, polyacrylate microspheres would be agglomerated if added directly in cement slurry and would not have the ability of sealing leaks due to the poor dispersing performance in cement slurry. The new core-shell OAM microspheres had broken this limit. The contact angle of core-shell OAM microspheres is 84.6° (Figure 11A) and the contact angle of polyacrylate microspheres is 120.3° (Figure 11B). The contact angle of polyacrylate microspheres is larger because polyacrylate was lipophilic. However, the contact angle of core-shell OAM microspheres is small, which is due to fumed silica shell combined with inner polyacrylate core, and the contact angle of core-shell OAM microspheres is near the contact angle of fumed silica particles. Comparing the contact angle of polyacrylate microspheres to that of core-shell OAM microspheres, core-shell OAM microspheres will have a better dispersion in cement slurry.

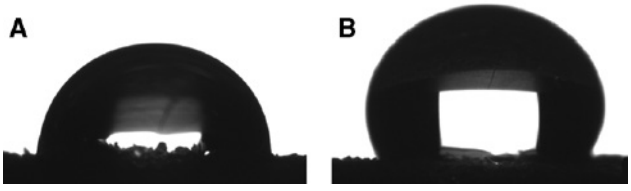

Figure 11: Contact angle images of core-shell OAM microspheres (A) and polyacrylate microspheres (B).

4 Conclusions

Core-shell OAM microspheres encapsulated with fumed silica shell were prepared using Pickering emulsion as a template. Modified fumed silica could stabilize Pickering polymerization because the extra silica in the bulk phase was adsorbed on the oil/water interface constantly when the oil droplets were deformed during polymerization. The increasing concentration of fumed silica could decrease the particle size of core-shell OAM microspheres and had little effect when the concentration was larger than 1 wt.%. However, the silica shell had negligible influence on the oil absorption rate on core-shell OAM microspheres. What's more, the silica shell made the surface of OAM microspheres hydrophilic and prevented polyacrylate from alkali hydrolyzing. Core-shell OAM microspheres may have excellent applications in oil well cement to realize the self-healing ability.

Because the oil well cementing condition is very harsh and the component of crude oil is complex, there is still a lot of work to do with self-healing materials. Considering that the temperature of many oil wells exceed 100°C, the high-temperature resistance and long-term effectiveness of core-shell OAM microspheres should be studied and enhanced. The oil absorption rate of core-shell OAM microspheres varies significantly for different oils; therefore, further research also needs to be done with OAM over special oil that is the main component of crude oil. Overall, our results offered a new avenue to prepare OAM microspheres based on the methodology of Pickering polymerization. We envision that this strategy would be an excellent solution to construct OAM microspheres, and more and more new materials absorbing oil will be developed using Pickering polymerization in this field.

Acknowledgments: This research work was supported by the National Basic Research Program of China (973 Program; 2015CB251202) and the Program for Changjiang Scholars and Innovative Research Team in University (No. IRT1086).

References

[1] Fang P, Mao PP, Chen J, Du Y, Hou X. *J. Appl. Polym. Sci.* 2014, 131, 40180.
[2] Ma LB, Cai N, Luo XG, Xue YN, Zhu S, Yu FQ. *Adv. Mater. Res.* 2013, 726, 658–661.
[3] Yang J, Shu WB, Qin W. *Acta Polym. Sin.* 2010, 7, 910–917.
[4] Wu B, Zhou MH. *J. Environ. Manage.* 2009, 90, 217–221.
[5] Aisien FA, Hymore FK, Ebewele RO. *Environ. Monit. Assess.* 2003, 85, 175–190.

[6] Ceylan D, Dogu S, Karacik B, Yakan SD, Okay OS, Okay O. *Environ. Sci. Technol.* 2009, 43, 3846–3852.
[7] Wu B, Zhou MH. *Waste Manage.* 2009, 29, 355–359.
[8] Liu XQ, Zhang G, Xing HQ, Huang P, Zhang XL. *Environ. Chem. Lett.* 2011, 9, 127–132.
[9] Grillo R, Pereira ADES, de Melo NFS, Porto RM, Feitosa LO, Tonello PS, Filho NLD, Rosa AH, Lima R, Fraceto LF. *J. Hazard. Mater.* 2011, 186, 1645–1651.
[10] Roy A, Singh SK, Bajpai J, Bajpai AK. *Cent. Eur. J. Chem.* 2014, 12, 453–469.
[11] Guo L, Zhu Y, Du X. *Starch – Stärke* 2012, 64, 552–562.
[12] Endo M, Noguchi T, Ito M, Takeuchi K, Hayashi T, Kim YA, Wanibuchi T, Jinnai H, Terrones M, Dresselhaus MS. *Adv. Funct. Mater.* 2008, 18, 3403–3409.
[13] Granger S, Loukili A, Pijaudier-Cabot G, Chanvillard G. *Cem. Concr. Res.* 2007, 37, 519–527.
[14] Termkhajornkit P, Nawa T, Yamashiro Y, Saito T. *Cem. Concr. Compos.* 2009, 31, 195–203.
[15] Wu M, Johannesson B, Geiker M. *Constr. Build. Mater.* 2012, 28, 571–583.
[16] Huang HL, Ye G, Damidot D. *Cem. Concr. Res.* 2013, 52, 71–81.
[17] Huang HL, Ye G, Shui ZH. *Constr. Build. Mater.* 2014, 63, 108–118.
[18] Thibodeaux K. *Alkali-Silica Reaction in Oilwell Cement Slurries Using Hollow Glass Spheres*. School of Civil and Environmental Engineering, Georgia Institute of Technology: USA, 2004.
[19] Wadsö L, Karlsson OJ. *Polym. Degrad. Stabil.* 2013, 98, 73–78.
[20] Möbius D, Miller R, Fainerman VB. *Surfactants: Chemistry, Interfacial Properties, Applications: Chemistry, Interfacial Properties, Applications*. Elsevier, 2001. Available at: https://www.elsevier.com/books/surfactants-chemistry-interfacial-properties-applications/m-bius/978-0-444-50962-8.
[21] Bon SAF, Cauvin S, Colver PJ. *Soft Matter.* 2007, 3, 194–199.
[22] He Y. *Mater. Lett.* 2005, 59, 114–117.
[23] Zhao Y, Yin G, Zheng Z, Wang H, Du Q. *J. Polym. Sci. Pt. A* 2011, 49, 5257–5269.
[24] Wang C, Zhang C, Li Y, Chen Y, Tong Z. *React. Funct. Polym.* 2009, 69, 750–754.
[25] Hu H, Wang H, Du Q. *Soft Matter.* 2012, 8, 6816–6822.
[26] Zhang K, Wu W, Meng H, Guo K, Chen JF. *Powder Technol.* 2009, 190, 393–400.
[27] Chen Y, Wang C, Chen J, Liu X, Tong Z. *J. Polym. Sci. Pt. A* 2009, 47, 1354–1367.
[28] Yang Y, Wei Z, Wang C, Tong Z. *ACS Appl. Mater. Interf.* 2013, 5, 2495–2502.
[29] Klonos P, Dapei G, Sulym IY, Zidropoulos S, Sternik D, Deryło-Marczewska A, Borysenko MV, Gun'ko VM, Kyritsis A, Pissis P. *Eur. Polym. J.* 2016, 74, 64–80.
[30] Sánchez-Flores NA, Pacheco-Malagón G, Pérez-Romo P, Armendáriz H, Valente JS, Guzmán-Castillo MDL, Alcaraz J, Baños L, Blesa JMS, Fripiat JJ. *J. Colloid Interf. Sci.* 2008, 323, 359–364.
[31] Pourjavadi A, Fakoorpoor SM, Khaloo A, Hosseini P. *Mater. Des.* 2012, 42, 94–101.
[32] Binks BP, Whitby CP. *Colloid Surf. A* 2005, 253, 105–115.
[33] Gun'ko VM, Turov VV, Krupska TV, Ruban AN, Kazanets AI, Leboda R, Skubiszewska-Zięba J. *J. Colloid Interf. Sci.* 2013, 394, 467–474.
[34] Klonos P, Sulym IY, Kyriakos K, Vangelidis I, Zidropoulos S, Sternik D, Borysenko MV, Kyritsis A, Deryło-Marczewska A, Gun'ko VM, Pissis P. *Polymer* 2015, 68, 158–167.
[35] Yan N, Gray MR, Masliyah JH. *Colloid Surf. A* 2001, 193, 97–107.
[36] Kostakis T, Ettelaie R, Murray BS. *Langmuir* 2006, 22, 1273–1280.
[37] Yang F, Liu SY, Xu J, Lan Q, Wei F, Sun DJ. *J. Colloid Interf. Sci.* 2006, 302, 159–169.
[38] Midmore BR. *Colloid Surf. A* 1998, 132, 257–265.
[39] Midmore BR. *Colloid Surf. A* 1998, 145, 133–143.
[40] Binks BP, Lumsdon SO. *Langmuir* 2000, 16, 8622–8631.
[41] Frelichowska J, Bolzinger MA, Chevalier Y. *J. Colloid Interf. Sci.* 2010, 351, 348–356.
[42] Abend S, Bonnke N, Gutschner U, Lagaly G. *Colloid Polym. Sci.* 1998, 276, 730–737.
[43] Thieme J, Abend S, Lagaly G. *Colloid Polym. Sci.* 1999, 277, 257–260.
[44] Abend S, Lagaly G. *Clay Miner.* 2001, 36, 557–570.
[45] Cheng S, Holt AP, Wang H. *Phys. Rev. Lett.* 2016, 116, 038302.
[46] Binks BP, Whitby CP. *Langmuir* 2004, 20, 1130–1137.
[47] Aveyard R, Binks BP, Clint JH. *Adv. Colloid Interf.* 2003, 100, 503–546.
[48] Wiley RM. *J. Colloid Sci.* 1954, 9, 427–437.
[49] Arditty S, Whitby CP, Binks BP, Schmitt V. *Eur. Phys. J. E* 2003, 11, 273–281.
[50] Arditty S, Schmitt V, Giermanska-Kahn J, Leal-Calderon F. *J. Colloid Interf. Sci.* 2004, 275, 659–664.
[51] Arditty S, Schmitt V, Lequeux F. *Eur. Phys. J. B* 2005, 44, 381–393.
[52] Midmore BR. *J. Colloid Interf. Sci.* 1999, 213, 352–359.
[53] Liu X, Wang YS, Yu HW, Wei Z, Liu NA. *Appl. Mech. Mater.* 2012, 209, 1199–1202.